IS-T 1829

Synthesis and Characterization of Novel Group VI Metal (Mo, W) Nitride and Oxide Compounds

by

Zhang, Zhihong

PHD Thesis submitted to Iowa State University

Ames Laboratory, U.S. DOE

Iowa State University

Ames, Iowa 50011

Date Transmitted: February 23, 1998

PREPARED FOR THE U.S. DEPARTMENT OF ENERGY

UNDER CONTRACT NO. W-7405-Eng-82.

DISCLAIMER

AVAILABILITY:

To DOE and DOE contractors: Office of Scientific and Technical Information
P.O. Box 62
Oak Ridge, TN 37831

prices available from: (615) 576-8401
FTS: 626-8401

To the public: National Technical Information Service
U.S. Department of Commerce
5285 Port Royal Road
Springfield, VA 22161

DISCLAIMER

Portions of this document may be illegible electronic image products. Images are produced from the best available original document.

Synthesis and characterization of novel Group VI metal (Mo, W) nitride and oxide compounds

Zhihong Zhang

Major Professor: Robert E. McCarley

Iowa State University

Binary Group VI metal nitrides are characterized by thermodynamic instability towards dissociation to N_2 and the N-saturated elements at high temperature. Our investigations into the preparation of tungsten nitrides have involved the synthesis of molecular precursors, and their conversion to tungsten nitrides at relatively low temperatures. Two interesting molecular precursors, $[WNCl_3 \cdot NCCH_3]_4$ and $WN(N_3)_3 \cdot xNCCH_3$, have been prepared and characterized. The molecular structure of $[WNCl_3 \cdot NCCH_3]_4$ consists of a W_4N_4 tetrameric core with multiple and single W-N bonds arranged in an alternating fashion. Three new solid state phases, amorphous W_3N_5, cubic WN, and $W_2N_2(C_2N_2)$, have been discovered by solid state and chemical vapor transport reactions. Cubic WN has a rock salt structure. $W_2N_2(C_2N_2)$ has a novel three-dimensional network structure consisting of W_2 dimers, hydrazido ligands N_2^{4-}, and 1,4-diazabutenido ligands represented by three resonance structures, [N-C=C-

$N]^{6-}$, $[N=C-C-N]^{6-}$, and $[N-C-C=N]^{6-}$.

Ternary reduced molybdenum oxides have caused great interest, since the discovery of $NaMo_4O_6$ containing trans-edge-shared Mo_6 octahedra. Recent investigations have yielded a new family of $LnMo_8O_{14}$ compounds containing cis- and trans-Mo_8 bicapped octahedra. A systematic study in the Ln_2O_3-MoO_3-Mo (Ln = La, Ce, Pr, Nd, Sm) system has been explored to better understand $LnMo_8O_{14}$. The study has shown that the sizes of the rare-earth cations affect the formation of these phases. Larger cations (La, Ce, and Pr) aid in the formation of trans-Mo_8 bicapped octahedra, and the smaller cations (Nd, Sm) only stabilize the cis-Mo_8 bicapped octahedra. Magnetic susceptibility measurements have indicated that no effective moment contribution arises from the Mo_8 metal clusters, even though the cis-Mo_8 cluster in $LnMo_8O_{14}$, containing all cis-Mo_8 octahedra, apparently contains an odd number of electrons (23). Electrical resistivity measurements and electronic structure calculations have shown that the $LnMo_8O_{14}$ compounds containing cis-Mo_8 clusters are metallic, and the $LnMo_8O_{14}$ compounds containing a 1:1 ratio of cis- to trans-Mo_8 clusters are semiconducting.

TABLE OF CONTENTS

Preprint — Removed for separate processing

Preprint — Removed for separate processing

Preprint — Removed for separate processing

LIST OF FIGURES

GENERAL INTRODUCTION

CHAPTER 1.

CHAPTER 2.

CHAPTER 3.

CHAPTER 4.

APPENDIX C.

LIST OF TABLES

APPENDIX A.

APPENDIX B.

APPENDIX D.

GENERAL INTRODUCTION

Group VI metal compounds have been the subject of much research since the discovery of the elements. Applications of these compounds vary widely from use in the alloying of steel[1] and as refractory materials (*e.g.*, WC for cutting tools and Mo_2Si for resistance heaters) to the iron-molybdenum cofactor in nitrogenase and endogenous tungsten in bacterial enzymes.[2] The many applications and uses of molybdenum and tungsten materials and their relative availability (1.2 ppm in the earth's crust) make them ideal candidates for scientific inquiry. This dissertation focuses on two areas of research on the chemistry of these two elements, the binary tungsten nitrides and the reduced molybdenum oxide compounds.

Group VI Metal (Mo, W) Nitrides

Traditional methods of preparing solid state materials required high temperatures in order to obtain diffusion rates necessary for the completion of the reactions. Thus, the number and types of compounds that can be prepared were restricted. This is especially true for the syntheses of materials which are thermodynamically less favorable at high temperatures. Therefore, "turning down the heat"[3] has become a popular topic in current solid state research. Many new technologies involving low temperature reactions (with respect to the traditional high temperature solid state

reactions), including flux,[4] hydrothermal,[5] intercalation,[6] and molecular precursor methods,[7] have been developed.

Transition metal nitrides possess free energies of formation that are dramatically less favorable than the corresponding oxides, principally because of the tremendous strength of the N≡N bond (227 kcal mol^{-1}) relative to O=O (119 kcal mol^{-1}). As a consequence, the preparation of transition metal nitrides is often entropically disfavored at high temperatures, and the number and types of transition metal nitrides are much less than that of the oxides.

An examination of the Group VI elements indicates a paucity of binary nitrides prepared by the traditional high temperature synthetic techniques, even though a number of ternary Group VI metal nitride compounds have been discovered.[8-14] Thermodynamic studies on Mo_2N by Lyutaya and Lakhtin demonstrated that the Gibbs free energy change for the formation of Mo_2N increased with the increase of temperature.[15-16] Table 1 lists some known and possible binary Group VI metal nitrides. Although considerable synthetic efforts have been devoted to preparing these nitride compounds, the structures and properties of these nitrides have remained elusive.[17-18] Only two types of Group VI metal nitrides were observed as bulk solid phases, MN and M_2N (M = Mo, W), with the metals in their lower oxidation states. Other phases are either unknown or prepared as thin films and observed only with electron microscopy. No bulk phases of Group VI metal nitrides with the metals in

Table 1. Some known and possible binary Group VI metal nitrides

Nitride	Example	Preparation	Structure
M_2N	Mo_2N, W_2N	M + NH_3 (800°C)	metal fcc, N random
M_3N_2	unknown		
MN	MoN, WN	M + NH_3 (700°C)	WC-hexagonal or hexagonal superlattice
M_4N_5	unknown		
M_3N_4	unknown		
M_2N_3	Mo_2N_3, W_2N_3		thin film-hexagonal
M_3N_5	W_3N_5		thin film-hexagonal
M_4N_7	unknown		
MN_2	WN_2		thin film-trigonal

oxidation states higher than III have ever been reported. WN_2, for example, was only observed as a brown coating on W filaments.[19] Mo_2N_3, which was prepared by the chemical vapor deposition (CVD) of $Mo(NMe_2)_4$ in ammonia gas, was also observed as a thin film.[20]

The bulk solid phases of the molybdenum and tungsten nitrides, MN and M_2N (M = Mo, W) with the metals in oxidation states lower than III, were prepared by flowing

NH_3 over the metals at high temperature. The mononitrides were reported to have the hexagonal WC structure. In the structures of M_2N, the metals were reported to be fcc close packed, where the nitrogen atoms are randomly located in octahedral interstitial positions.[21]

Since the problems in traditional synthetic methodologies have limited the number and types of transition metal nitride compounds, new synthetic techniques of converting molecular precursors to the target products under more gentle conditions have been explored.[7] Parkin and co-workers attempted to convert metal halides to nitrides, which was successful for most early transition metals, but not for the Group VI metals.[22] They attempted to convert $MoCl_3$ and WCl_4 to the nitrides by reaction with magnesium or calcium nitride at 500 °C. However, only the metals were obtained.

Similarly, our synthetic strategy to produce binary Group VI metal nitrides involved the conversion of molecular precursors to the metal nitrides. However, our preferred molecular precursors are $MNCl_3$ (M = Mo, W), which can be prepared from the reaction of trimethylsilyl azide with $MoCl_5$ or WCl_6 in 1,1-dichloromethane or 1,2-dichloroethane, respectively. $MNCl_3$ represents a potential intermediate to the desired products MN_x ($x \geq 1$). Through metathesis or redox reactions, Cl atoms could be replaced by other ligands, such as N_3^-, N_2^{4-}, and N^{3-}, or removed by reduction reactions.

In this dissertation, new molecular precursors to tungsten nitrides are reported. Several new tungsten nitrides and carbide nitrides with novel structures, which were synthesized by metathetical reactions in a flux, thermal decomposition of the molecular precursors at relatively low temperatures, or by chemical vapor transport reactions, will be reported as well.

Ternary Reduced Molybdenum Oxides

Since the discovery of the reduced molybdenum oxide, $NaMo_4O_6$,[23] containing trans-edge-shared Mo_6 octahedra (Figure 1), ternary reduced molybdenum oxides have been studied extensively. A large number of compounds have been synthesized which contain various kinds of condensed Mo metal clusters.[24] Over the past several years, ternary reduced rare-earth molybdenum oxides have caused great interest, because these compounds may possess interesting electrical and magnetic properties. Many compounds have been discovered in this area, and most of them have been structurally characterized.[25-32]

One interesting family of ternary reduced rare-earth molybdenum oxides is the group of compounds containing Mo_8 bicapped octahedra. The Mo_8 bicapped octahedra could have three structural isomers (cis-, meta-, and trans-), which are shown in Figure 2. This structural feature may lead to an interesting crystal structure chemistry, because any combination of these isomers would generate a new crystal

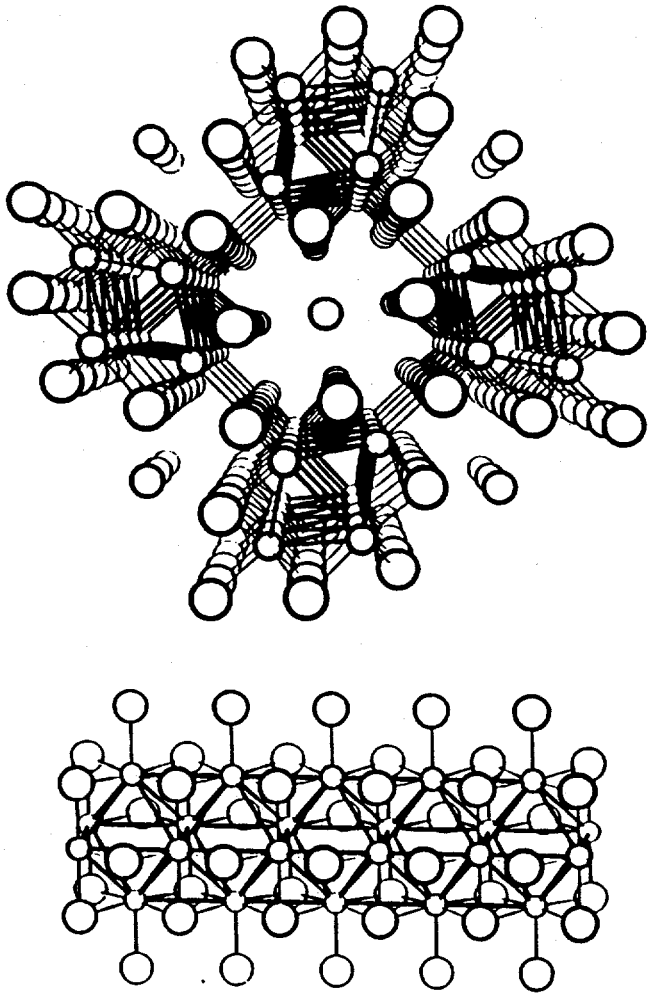

Figure 1. The structure of $NaMo_4O_6$ viewed down the tetragonal c axis and a segment of a single chain of trans-edge-shared Mo_6O_{12}-type clusters extended parallel to the c axis.

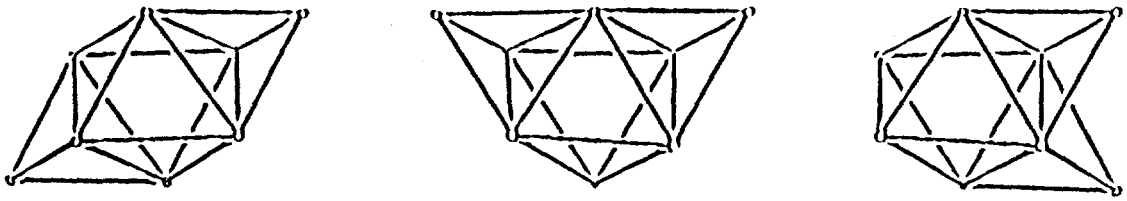

Trans- Meta- Cis-

Figure 2. The three structural isomers of Mo_8 bicapped octahedra.

structure type.

The first compound containing Mo_8 bicapped octahedra was synthesized by electrolysis in 1990.[33] This compound has a non-stoichiometric formula, $LaMo_{7.7}O_{14}$, and contains only cis-bicapped Mo_8 octahedra, in which the face-capping positions are only 85% occupied by the Mo atoms. Subsequently, a stoichiometric compound, $NdMo_8O_{14}$,[34] was discovered, in which the face-capping positions are fully occupied. These compounds exhibit paramagnetic behavior over the temperature range of 100-300K, and metallic character at room temperature.[35-36]

More recently, the $CeMo_8O_{14}$[37] and $PrMo_8O_{14}$[38] compounds, which contain 1:1 and 2:1 ratios of cis- to trans-bicapped Mo_8 octahedra, respectively, have been

prepared at extremely high temperatures by P. Gougeon and coworkers.

In this work, the $LnMo_8O_{14}$ compounds (Ln = rare-earth) containing Mo_8 bicapped octahedra have been systematically studied. The synthetic conditions, X-ray powder diffraction, single crystal structure determinations, electronic structure calculations, and properties of these interesting compounds will be discussed.

Dissertation Organization

This dissertation consists of four papers. Each paper is formatted for publication in a technical journal and the cited references are found at the end of each paper. GENERAL CONCLUSIONS follow the four papers. The references cited in the GENERAL INTRODUCTION are found at the end of the dissertation.

GENERAL CONCLUSIONS

The goal of this dissertation has been to develop the chemistry of Group VI metal (Mo, W) nitrides and oxides.

When compared to their oxides, much less information is known about the Group VI nitrides. This lack of information stems from the chemical instability of Group VI metal nitrides with respect to N_2 and N-saturated elements at high temperatures. Therefore, "turning down the heat" has become an important synthetic strategy to produce Group VI metal nitrides. One focus of this dissertation was to prepare tungsten nitrides via molecular precursors at relatively low temperatures.

$WNCl_3$, which contains a tetrameric nitride core W_4N_4, represents a potential intermediate to the desired product WN_x ($x \geq 1$). It is soluble in acetonitrile and forms an acetonitrile adduct $[WNCl_3 \cdot NCCH_3]_4$. The $[WNCl_3 \cdot NCCH_3]_4$ complex consists of a W_4N_4 tetrameric core as well. Substitution of chloride by nitride and azide has been accomplished by either solid state reactions or solution reactions at low temperatures. Several new nitrides and carbide nitrides have been prepared and characterized. However, attempts to remove chlorine by reduction reaction, using reducing reagents such as hexamethyldisilane, tributyltin hydride, tin and zinc metal, were not successful.

An interesting compound $WN(N_3)_3$ was prepared from the reaction of $WNCl_3$ and

NaN_3 in acetonitrile at room temperature. It may have a similar tetrameric structure to $[WNCl_3 \cdot NCCH_3]_4$. Due to the extremely explosive nature, this compound could not be isolated from the acetonitrile solution in a large yield. Thermal decomposition of this compound in 1,2-dichlorobenzene at reflux was attempted, however, the azide did not decompose completely.

A bulk solid phase of tungsten nitride W_3N_5 was prepared through a solid state reaction between $WNCl_3$ and Zn_3N_2 in sealed Pyrex tubes at 400 °C. The XPS study indicated that the oxidation state of tungsten in this amorphous phase was +5. Therefore, each tungsten atom in this W_3N_5 compound possesses one single d-electron. The magnetic susceptibility measurements indicated that W_3N_5 exhibited diamagnetic property in the temperature range 6-300 K. This result suggest that the single electron possessed by the tungsten atom in W_3N_5 be used for W-W bond formation.

By heating W_3N_5 at 600°C in sealed quartz tubes, a cubic tungsten mononitride phase (WN) with rock salt structure (a = 4.171 Å) was obtained. Similarly, by heating W_3N_5 at 800 °C in sealed quartz tubes the hexagonal WN phase and tungsten metal were obtained. At the same time, a few golden crystals were also obtained, which were grown via a chemical transport reaction. The structure of the golden compound $W_2N_2(C_2N_2)$ consists of W_2 dimers, hydrazido ligands N_2^{4-}, and 1,4-diazabutenido ligands represented by three resonance structures, $[N\text{-}C{=}C\text{-}N]^{6-}$, $[N{=}C\text{-}C\text{-}N]^{6-}$, and $[N\text{-}C\text{-}C{=}N]^{6-}$. The dimers are linked together by μ^2, η^2 N-N and N-C-C-N groups to

form a 3-dimensional network. The metal to hydrazido nitrogen bond distances fall in the range 1.97(4) to 2.19(4) Å, and the metal-diazabutenido nitrogen distances show a more limited range from 2.01(4) to 2.07(3) Å. The hydrazido N-N bond distance is 1.43(5) Å, and the diazabutenido C-C bond distance is 1.59(4) Å and N-C bond distance 1.56(4) Å. The W-W single bond distance is 2.767(2) Å.

The electronic structure calculations indicated that the cubic WN with NaCl structure was a conductor and might exhibit superconductivity because the high density of states at the Fermi level. However, the magnetic susceptibility measurements indicated that the cubic WN was basically diamagnetic above 6 K, but did not show any evidence that this cubic WN phase was a superconductor.

The reduced ternary molybdenum oxides have been extensively explored since the discovery of the $NaMo_4O_6$ compound containing trans-edge-shared Mo_6 octahedra. Many compounds with interesting structures and properties have been found.

A new reduced ternary rare-earth molybdenum oxide $LaMo_8O_{14}$ containing Mo_8 bicapped octahedra was discovered at 1250°C in a sealed, evacuated quartz tube. The novel structure contains a 1:1 ratio of cis- to trans-Mo_8 bicapped octahedra, which are arranged alternately along the c-axis of the unit cell. The Mo-Mo bond distances are in the range of 2.590(4) to 2.888(6) Å. The average Mo-Mo bond distance in the trans-isomer is 2.703 Å, which is shorter than that found in the cis-isomer (2.748 Å). The Mo-O bond distances are in the range of 1.94(3) to 2.18(2) Å. The Mo-O bond

strength calculations indicate that the cis- and trans-Mo_8 clusters in $LaMo_8O_{14}$ contain 22 and 24 electrons, respectively.

A systematic investigation in the Ln_2O_3-MoO_3-Mo (Ln = La, Ce, Pr, Nd, Sm) system was explored at 1250°C in sealed, evacuated quartz tubes. Under these synthetic conditions, only the phases containing all cis-Mo_8 bicapped clusters, and a 1:1 ratio of cis-Mo_8 to trans-Mo_8 bicapped clusters, were found. However, the phase containing a 2:1 ratio of cis- to trans-Mo_8 bicapped octahedra was not observed. It was noteworthy that the sizes of the rare-earth cations were critical for the formation of the various phase types. The larger cations (La, Ce, and Pr) aided in the formation of trans-Mo_8 octahedra, and the smaller cations (Nd and Sm) only stabilized the cis-Mo_8 octahedra. A rational explanation for this result arises from the observation that the effective volume of cis-Mo_8 cluster is 3/4th the value of the trans-Mo_8 cluster. The magnetic susceptibility measurements indicate that no effective moment contribution arises from the metal clusters Mo_8, even though the cis-Mo_8 cluster in $LnMo_8O_{14}$ containing all cis-Mo_8 octahedra should contain an odd number of electrons (23 e^-). The electrical resistivity measurements and electronic structure calculations indicate that the $LnMo_8O_{14}$ containing all cis-Mo_8 clusters are metallic compounds, and the $LnMo_8O_{14}$ containing a 1:1 ratio of cis- to trans-Mo_8 clusters are semiconducting compounds.

APPENDIX A. PHYSICAL CONSTANTS

Table A-1. Values of physical constants involved in this dissertation[a]

Quantity	Symbol	Value	Units
Planck constant	h	6.6260755(40)	10^{-34} J s
Bohr magneton	μ_B	9.2740154(31)	10^{-24} J T^{-1}
Avogadro constant	N_A	6.0221367(36)	10^{23} mol^{-1}
Boltzmann constant	k	1.380658(12)	10^{-23} J K^{-1}

[a] Alberty, R. A.; Silbey, R. J. *Physical Chemistry*, 1st Ed. John Wiley & Sons, Inc. New York, **1992**.

APPENDIX B. CORE-DIAMAGNETIC SUSCEPTIBILITIES

Table B-1. Selected core-diamagnetic susceptibilities[a]

Ion	Susceptibility	
	-1.0×10^{-6} emu/g	-1.0×10^{-4} emu/mol
Ag^{+}	24	25.89
Cd^{2+}	22	24.73
Ce^{3+}	20	28.02
Ce^{4+}	17	23.82
Cl^{-}	26	9.23
CN^{-}	18	4.68
Cu^{+}	12	7.63
Cu^{2+}	11	6.99
Dy^{3+}	19	30.88
Er^{3+}	18	30.11
Eu^{2+}	22	33.43
Eu^{3+}	20	30.39
F^{-}	11	2.09
Fe^{2+}	13	7.26
Fe^{3+}	10	5.58
Gd^{3+}	20	31.45
Hf^{4+}	16	28.56
Hg^{2+}	37	74.22

Table B-1. (continued)

Ho^{3+}	19	31.34
O^{2-}	12	1.92
OH^-	12	2.04
La^{3+}	20	27.78
Lu^{3+}	17	29.74
Mo^{2+}	31	29.74
Mo^{3+}	23	22.07
Mo^{4+}	17	16.31
Mo^{5+}	12	11.51
Mo^{6+}	7	67.16
Nd^{3+}	20	28.85
NH_4^+	11.5	1.73
Pr^{3+}	20	28.18
Pr^{4+}	17	23.95
Sc^{3+}	6	2.70
Sm^{2+}	23	34.59
Sm^{3+}	20	30.08
Sn^{2+}	20	23.74
Sn^{4+}	16	18.99
Sr^{2+}	15	13.14
Ta^{5+}	14	25.33
Tb^{3+}	19	30.20
Tb^{4+}	17	27.02
Te^{2-}	70	89.32
Te^{4+}	14	17.86

Table B-1. (continued)

Te^{6+}	12	15.31
Th^{4+}	23	53.37
Ti^{3+}	9	4.31
Ti^{4+}	5	2.40
Tl^{+}	34	69.49
Tl^{3+}	31	63.35
Tm^{3+}	18	30.41
V^{2+}	15	7.64
V^{3+}	10	5.09
V^{4+}	7	3.57
V^{5+}	4	2.04
W^{2+}	41	75.38
W^{3+}	36	66.19
W^{4+}	23	42.29
W^{5+}	19	34.93
W^{6+}	13	23.90
Y^{3+}	12	10.67
Yb^{2+}	20	34.61
Yb^{3+}	18	31.15

[a] Mulay, L. N.; Boudreaux, E. A. *Theory and applications of molecular diamagnetism*, New York: Wiley, **1976**.

APPENDIX C. MAGNETIC PROPERTIES OF Ln_2O_3

The molar magnetic susceptibilities of Ln_2O_3 (Ln = La, Pr, Nd, and Sm) as a function of temperature are shown in the following Figures. The susceptibility data in the 100-300 K range were fit to a modified Curie-Weiss relationship, $\chi = C/(T - \theta) + \chi_o$, where C, θ, and χ_o refer to the Curie constant, the Weiss temperature, and temperature independent susceptibility.

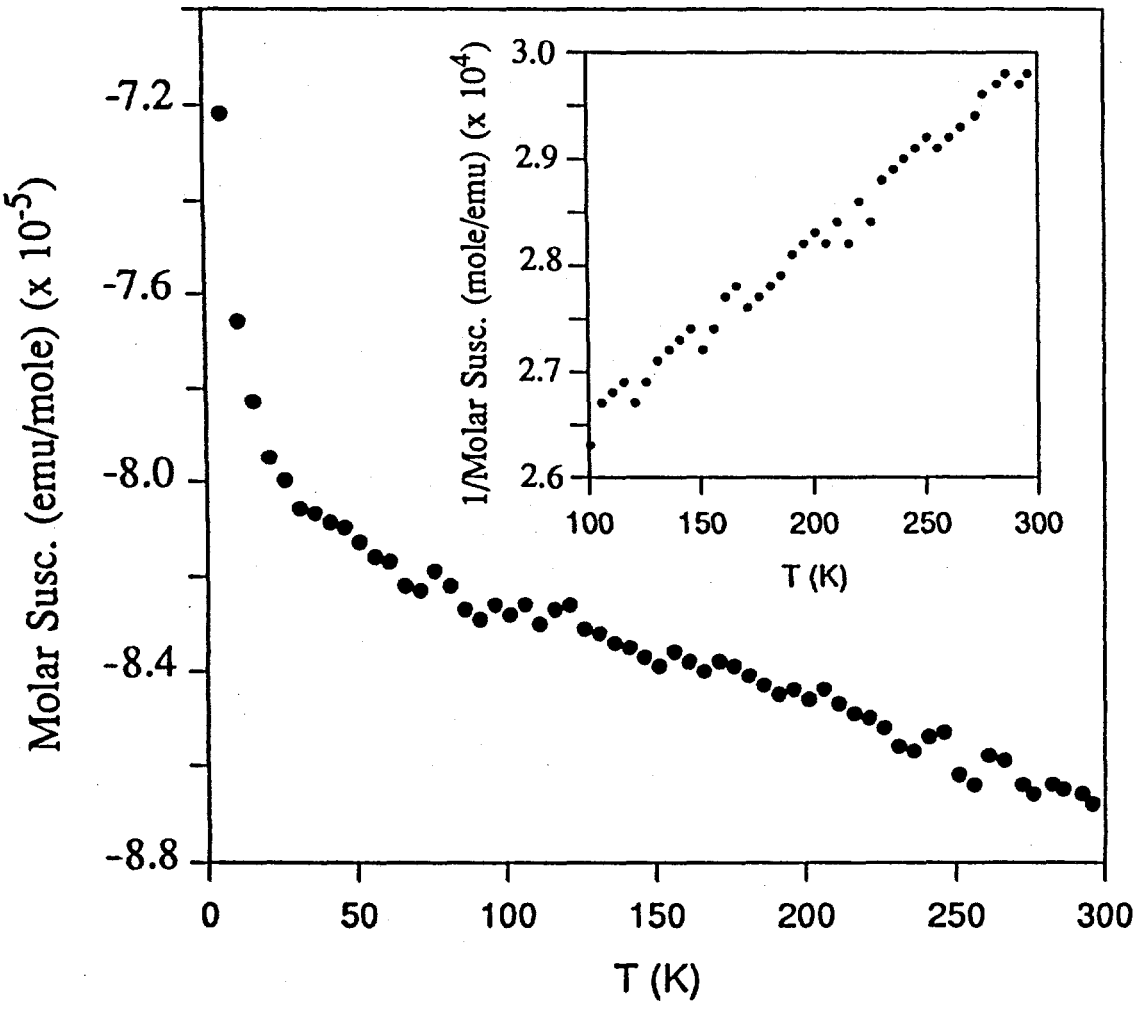

Figure C-1. The molar magnetic susceptibility of La_2O_3 as a function of temperature and reciprocal susceptibility vs. temperature (inset).

Curie = 0.059, Weiss = -39.1, χ_o = -1.2 x 10^{-4}, and μ = 0.69.

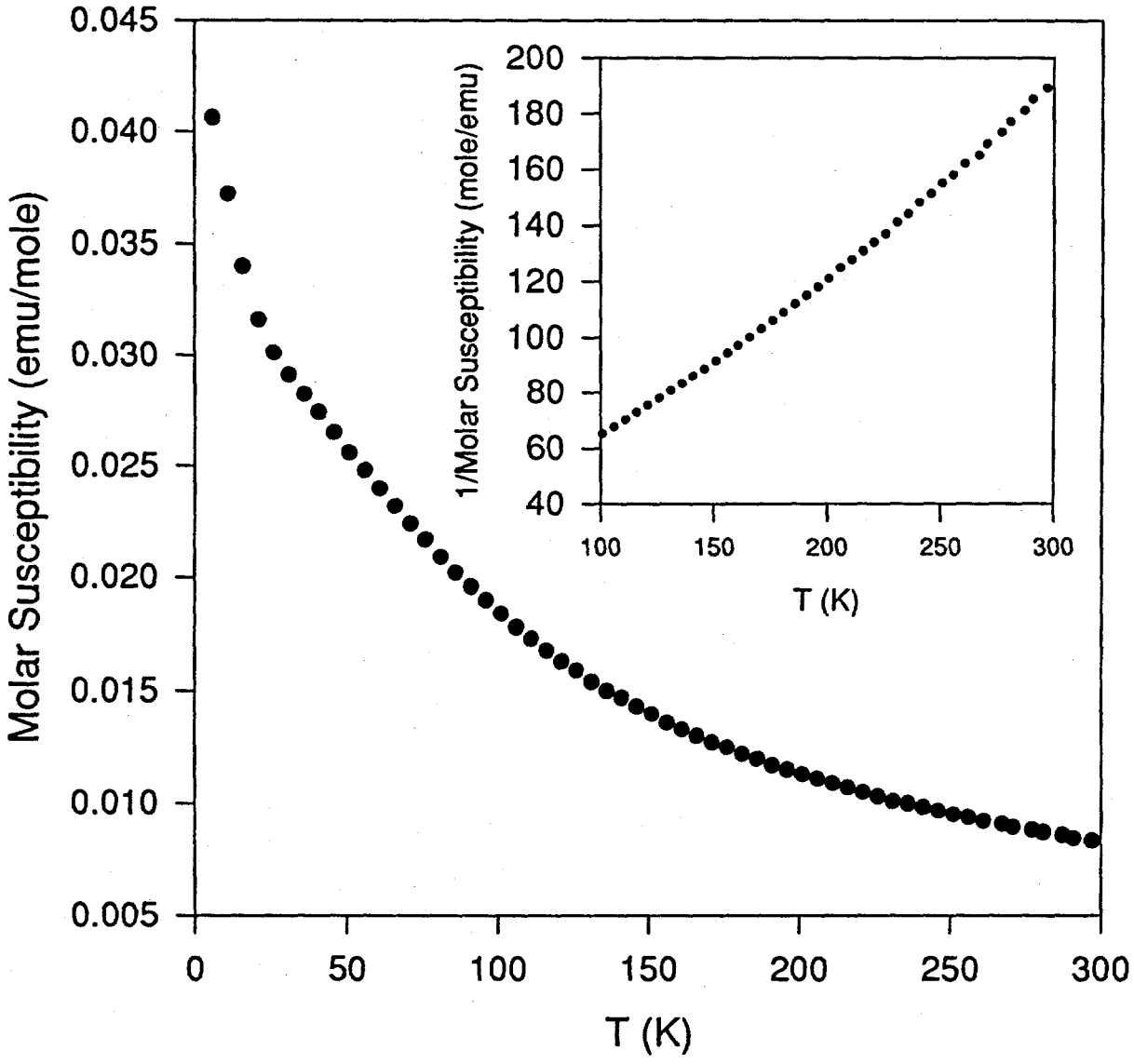

Figure C-2. The molar magnetic susceptibility of Pr_2O_3 as a function of temperature and reciprocal susceptibility vs. temperature (inset).

Curie = 1.59, Weiss = -2.7, χ_o = 3.04 x 10^{-3}, and μ = 3.57.

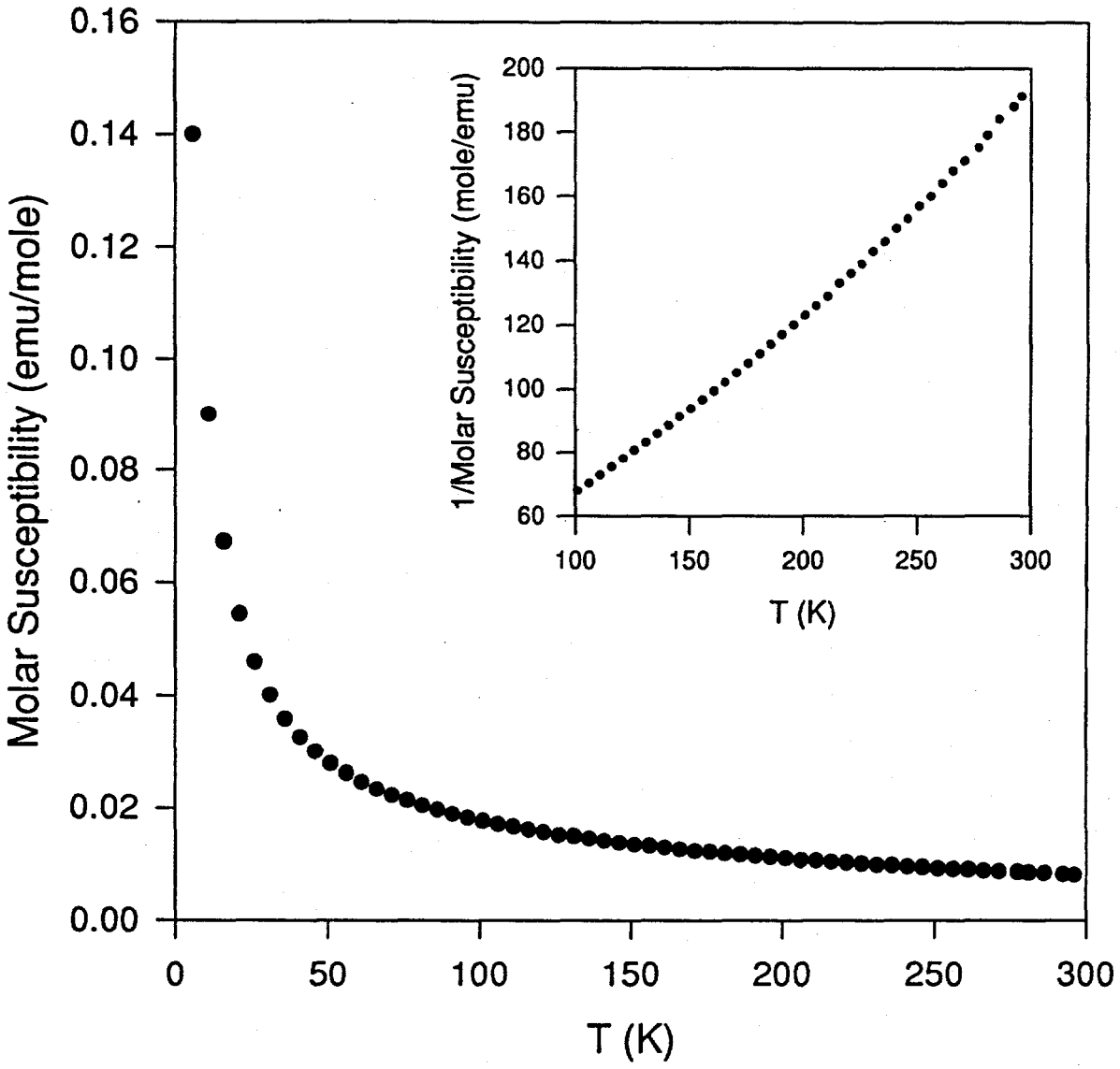

Figure C-3. The molar magnetic susceptibility of Nd_2O_3 as a function of temperature and reciprocal susceptibility vs. temperature (inset).
Curie = 1.59, Weiss = -0.51, χ_o = 2.83 x 10^{-3}, and μ = 3.57.

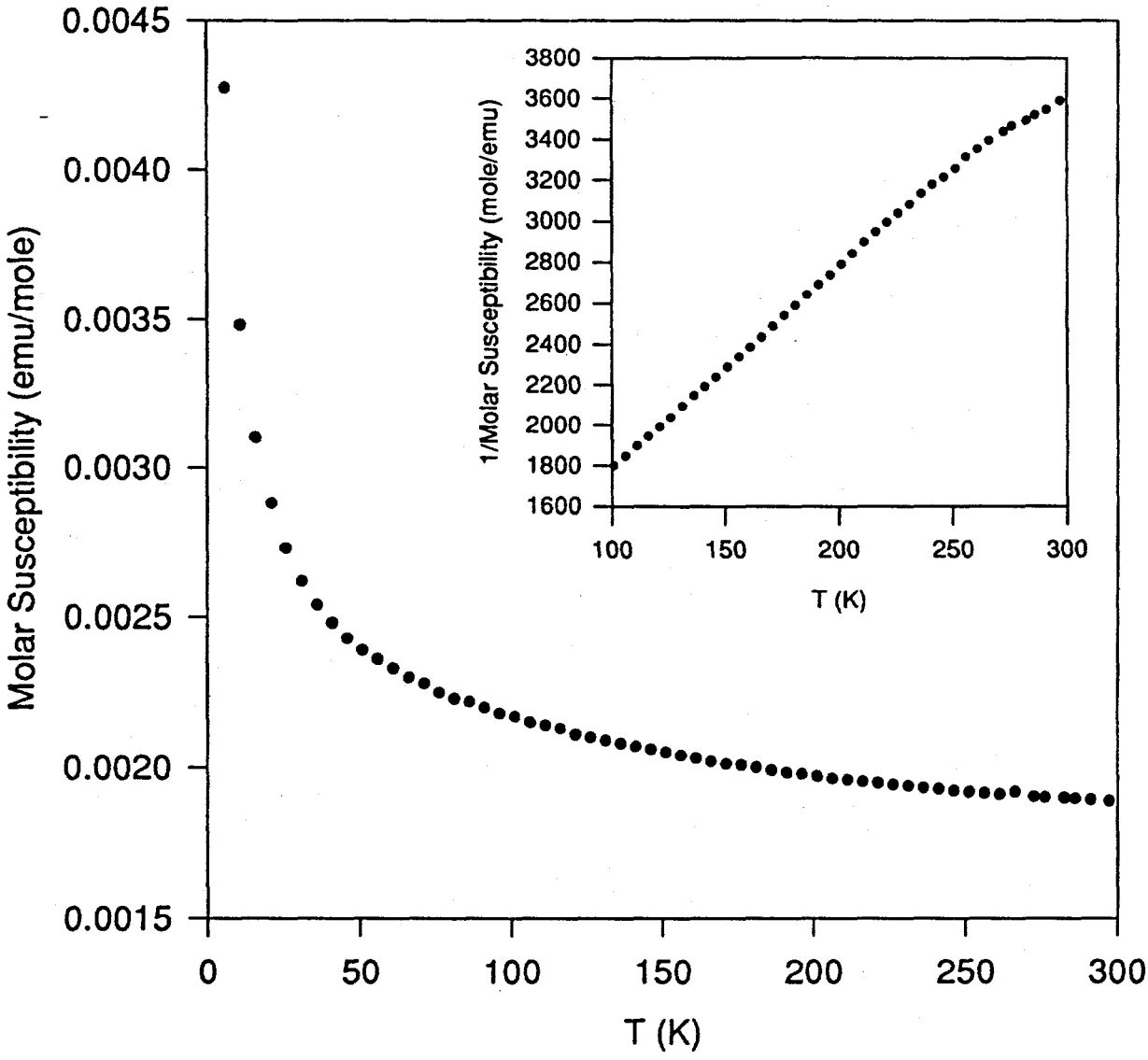

Figure C-4. The molar magnetic susceptibility of Sm_2O_3 as a function of temperature and reciprocal susceptibility vs. temperature (inset).

Curie = 0.11, Weiss = -92.5, χ_o = 1.16 x 10^{-3}, and μ = 0.94

APPENDIX D. $[WNCl_3 \cdot NCCH_2CH_3]_4$

X-ray structure determination

The single crystals of $[WNCl_3 \cdot NCCH_2CH_3]_4$ were obtained by dissolving $[WNCl_3 \cdot NCCH_2CH_3]_4$ in 1,1-dichloromethane and standing at room temperature for two weeks. A suitable deep orange single crystal with dimensions 0.20 x 0.10 x 0.10 mm^3 was selected from material still in contact with the mother solution. The crystal was then encased in epoxy resin while in a glove bag under a nitrogen flow, attached to the tip of a glass fiber, and immediately delivered to the diffractometer with low temperature equipments. All measurements were made on a Rigaku AFC6R diffractometer using graphite monochromated Mo Kα (λ = 0.71069 Å) radiation and a 12 kW rotating anode generator.

Cell constants and an orientation matrix for data collection were obtained from a least-squares refinement using the setting angles of 25 carefully centered reflections in the range $4.0 < 2\theta < 35.0$, and corresponded to a triclinic cell with dimensions: a = 8.875(2) Å, b = 10.220(2) Å, c = 10.311(2) Å, α = 110.76(1)°, β = 92.36(1)°, γ = 89.56(1)°, and V = 873.7(3) $Å^3$. The data were collected at -60 °C using the ω-2θ scan technique over the range $4° < 2\theta < 50°$ in the hemisphere ($\pm h$, $+k$, $\pm l$). Three standard reflections were monitored every 150 reflections and showed no intensity variation over the collection period. A total of 3283 reflections were collected, of

which 3092 were unique (R_{int} = 0.024) and 2644 of which were observed with $I > 3.00\sigma(I)$. No Decay correction was applied. With an absorption coefficient for Mo Kα radiation of μ = 140.7 cm^{-1}, an empirical absorption correction using the ψ scan technique was applied after the structure solution. The data were corrected for Lorentz and polarization effects.

The triclinic space group was $P\bar{1}$ (#2) was chosen on the basis of systematic absences and intensity statistics. The structure was solved by the SHELXS direct methods which yielded the positions of the tungsten atoms. Successive Fourier electron difference maps yielded the positions of the chlorine, nitrogen and carbon atoms. The structure was then refined by full-matrix least-squares methods with anisotropic thermal parameters on all non-hydrogen atoms. The final cycle of full-matrix least-squares refinement was based on 2644 observed reflections and 163 variable parameters and converged with unweighted and weighted agreement factors of R = 0.023 and Rw = 0.031, respectively. The asymmetric unit was found to be $[WNCl_3 \cdot NCCH_2CH_3]_2$. All calculations were performed using the TEXSAN crystallographic software package of Molecular Structure Corporation. The crystallographic data and refinement results are given in Table D-1, and the positional parameters and isotropic equivalent temperature factors are given in Table D-2. The anisotropic temperature factors are listed in Table D-3.

Table D-1. Crystallographic data for $[WNCl_3 \cdot NCCH_2CH_3]_4$

Empirical Formula	$C_{12}Cl_{12}H_{20}N_8W_4$
Formula Weight	1437.18
Crystal Size	0.20 x 0.10 x 0.10 mm^3
Crystal System	triclinic
Space Group	P1 (#2)
Lattice Parameters	a = 8.875(2) Å
	b = 10.311(2) Å
	c = 10.220(2) Å
	α = 110.76(1)°
	β = 92.36(1)°
	γ = 89.56(1)°
Volume	873.7(3) $Å^3$
Z Value	1
Calculated Density	2.731 g/cm^3
F_{000}	648.00
μ(MoKα)	140.74 cm^{-1}
Diffractometer	Rigaku AFC6R
Radiation	MoKα (λ = 0.71069Å)
Temperature	-60.0 °C
Two-theta Range	0-50°
Scan Mode	ω-2θ
No. of Reflections Collected	3283
No. Observations (I > 3.00σ(I))	2644
No. Variables	163
Max Shift/error in Final Cycle	0.00
Goodness of Fit[a]	2.56
Max. and Min. Peaks in the Final Diff. Map	0.86, -1.55 $e^-/Å^3$
Residuals[b]	R = 0.023, Rw = 0.031

[a] Goodness of Fit = $[\Sigma\omega\{|F_o| - |F_c|\}^2/\{N_{obs} - N_{parameters}\}]^{1/2}$

[b] $R = \Sigma \; | \; |Fo| - |Fc| \; | \; / \; \Sigma \; |Fo|$; $Rw = [(\Sigma \; w \; (|Fo| - |Fc|)^2 \; / \; \Sigma \; w \; Fo^2)]^{1/2}$.

Table D-2. Atomic coordinates and equivalent isotropic thermal parameters ($Å^2$) of the non-hydrogen atoms for $[WNCl_3 \cdot NCCH_2CH_3]_4$

atom	x	y	z	B_{eq} [a]
W(1)	0.35810(4)	-0.75580(3)	0.56381(3)	1.293(8)
W(2)	0.70306(4)	-0.88754(3)	0.70801(3)	1.275(7)
Cl(1)	0.5359(3)	-0.6904(2)	0.4407(2)	2.42(5)
Cl(2)	0.8675(3)	-0.8488(3)	0.5590(3)	2.61(5)
Cl(3)	0.2348(3)	-0.7890(3)	0.7749(2)	2.44(5)
Cl(4)	0.7751(3)	-0.6930(2)	0.8979(3)	2.96(5)
Cl(5)	0.1703(3)	-0.6206(2)	0.5202(3)	2.78(5)
Cl(6)	0.5806(3)	-0.9850(2)	0.8504(2)	2.22(5)
N(1)	0.3181(8)	-0.9123(7)	0.4385(7)	1.6(2)
N(2)	0.5461(7)	-0.8260(7)	0.6493(7)	1.6(1)
N(3)	0.4478(9)	-0.5518(7)	0.7428(8)	2.3(2)
N(4)	0.9178(9)	-0.9910(8)	0.7740(8)	2.5(2)
C(1)	0.511(1)	-0.4606(10)	0.8177(10)	2.1(2)
C(2)	1.025(1)	-1.042(1)	0.7908(10)	2.5(2)
C(3)	0.591(1)	-0.339(1)	0.916(1)	3.2(2)
C(4)	1.165(1)	-1.113(1)	0.813(1)	3.1(2)
C(5)	0.749(1)	-0.326(1)	0.869(1)	3.7(3)
C(6)	1.144(1)	-1.270(1)	0.765(1)	3.6(3)

[a] $B_{eq} = 8/3\pi^2(U_{11}(aa^*)^2 + U_{22}(bb^*)^2 + U_{33}(cc^*)^2 + 2U_{12}aa^*bb^*\cos\gamma + 2U_{13}aa^*cc^*\cos\beta + 2U_{23}bb^*cc^*\cos\alpha)$

Table D-3. Anisotropic thermal parameters[a] ($Å^2$) of the non-hydrogen atoms for $[WNCl_3 \cdot NCCH_2CH_3]_4$

Atom	U_{11}	U_{22}	U_{33}	U_{12}	U_{13}	U_{23}
W(1)	0.0162(2)	0.0170(2)	0.0157(2)	-0.0013(1)	-0.0009(1)	-0.0058(1)
W(2)	0.0152(2)	0.0165(2)	0.0169(2)	-0.0022(1)	0.0002(1)	-0.0064(1)
Cl(1)	0.033(1)	0.032(1)	0.034(1)	0.006(1)	0.002(1)	-0.019(1)
Cl(2)	0.023(1)	0.038(1)	0.046(1)	0.003(1)	0.003(1)	-0.025(1)
Cl(3)	0.025(1)	0.024(1)	0.043(1)	0.0026(9)	0.006(1)	-0.011(1)
Cl(4)	0.044(2)	0.033(1)	0.027(1)	-0.013(1)	0.005(1)	-0.002(1)
Cl(5)	0.030(1)	0.042(1)	0.032(1)	-0.007(1)	-0.011(1)	-0.012(1)
Cl(6)	0.032(1)	0.025(1)	0.032(1)	0.0046(10)	0.0002(10)	-0.016(1)
N(1)	0.019(4)	0.019(4)	0.023(4)	-0.004(3)	0.001(3)	-0.008(3)
N(2)	0.014(4)	0.028(4)	0.019(3)	0.001(3)	-0.002(3)	-0.010(3)
N(3)	0.035(5)	0.032(5)	0.016(4)	-0.007(4)	0.001(4)	-0.006(4)
N(4)	0.023(4)	0.033(5)	0.035(5)	-0.004(4)	-0.004(4)	-0.010(4)
C(1)	0.025(5)	0.023(5)	0.034(5)	0.003(4)	-0.005(4)	-0.014(4)
C(2)	0.024(5)	0.023(5)	0.043(6)	-0.004(4)	-0.004(5)	-0.008(5)
C(3)	0.041(6)	0.040(7)	0.033(6)	-0.002(5)	0.014(5)	-0.001(5)
C(4)	0.028(6)	0.046(7)	0.039(6)	-0.011(5)	-0.012(5)	-0.012(5)
C(5)	0.039(7)	0.043(7)	0.057(7)	0.001(5)	0.019(6)	-0.015(6)
C(6)	0.036(6)	0.064(8)	0.046(7)	0.006(6)	-0.010(5)	-0.028(6)

[a]The coefficients U_{ij} of the anisotropic temperature factor expression are defined as $\exp(-2\pi^2(a^{*2}U_{11}h^2 + b^{*2}U_{22}k^2 + c^{*2}U_{33}l^2 + 2a^*b^*U_{12}hk + 2a^*c^*U_{13}hl + 2b^*c^*U_{23}kl))$

Description of structure

$[WNCl_3 \cdot NCCH_2CH_3]_4$ crystallizes in the triclinic space group $P\bar{1}$ with one $[WNCl_3 \cdot NCCH_2CH_3]_4$ molecule per unit cell. There are no free solvent molecules in the unit cell. An ORTEP diagram of the unit cell is shown in Figure D-1. The molecular structure of $[WNCl_3 \cdot NCCH_3CH_3]_4$ (Figure D-2), which is similar to the molecular structure of $[WNCl_3 \cdot NCCH_3]_4$, consists of a W_4N_4 tetramer core. The selected bond distances and angles for $[WNCl_3 \cdot NCCH_2CH_3]_4$ are listed in Tables D-4 and D-5, respectively.

Table D-4. Selected bond distances (Å) in $[WNCl_3 \cdot NCCH_2CH_3]_4$

atom	atom	distance	atom	atom	distance
W(1)	Cl(1)	2.304(2)	W(1)	Cl(3)	2.315(2)
W(1)	Cl(5)	2.294(2)	W(1)	N(1)	1.696(7)
W(1)	N(2)	2.093(6)	W(1)	N(3)	2.362(7)
W(2)	Cl(2)	2.288(2)	W(2)	Cl(4)	2.315(2)
W(2)	Cl(6)	2.344(2)	W(2)	N(1)	2.080(7)
W(2)	N(2)	1.700(6)	W(2)	N(4)	2.366(7)
N(3)	C(1)	1.12(1)	N(4)	C(2)	1.12(1)
C(1)	C(3)	1.47(1)	C(2)	C(4)	1.49(1)
C(3)	C(5)	1.52(1)	C(4)	C(6)	1.53(1)

Table D-5. Selected bond angles (°) in $[WNCl_3 \cdot NCCH_2CH_3]_4$

atom	atom	atom	angle	atom	atom	atom	angle
Cl(1)	W(1)	Cl(3)	161.80(8)	Cl(1)	W(1)	Cl(5)	94.86(9)
Cl(1)	W(1)	N(1)	96.0(3)	Cl(1)	W(1)	N(2)	83.5(2)
Cl(1)	W(1)	N(3)	81.3(2)	Cl(3)	W(1)	Cl(5)	93.75(9)
Cl(3)	W(1)	N(1)	97.9(3)	Cl(3)	W(1)	N(2)	83.7(2)
Cl(3)	W(1)	N(3)	83.3(2)	Cl(5)	W(1)	N(1)	101.1(2)
Cl(5)	W(1)	N(2)	163.6(2)	Cl(5)	W(1)	N(3)	86.4(2)
N(1)	W(1)	N(2)	94.7(3)	N(1)	W(1)	N(3)	171.7(3)
N(2)	W(1)	N(3)	77.3(3)	Cl(2)	W(2)	Cl(4)	95.04(10)
Cl(2)	W(2)	Cl(6)	162.85(8)	Cl(2)	W(2)	N(1)	86.0(2)
Cl(2)	W(2)	N(2)	97.2(2)	Cl(2)	W(2)	N(4)	82.3(2)
Cl(4)	W(2)	Cl(6)	92.15(9)	Cl(4)	W(2)	N(1)	164.4(2)
Cl(4)	W(2)	N(2)	100.0(2)	Cl(4)	W(2)	N(4)	84.8(2)
Cl(6)	W(2)	N(1)	83.0(2)	Cl(6)	W(2)	N(2)	96.8(2)
Cl(6)	W(2)	N(4)	82.9(2)	N(1)	W(2)	N(2)	95.2(3)
N(1)	W(2)	N(4)	80.0(3)	N(2)	W(2)	N(4)	175.2(3)
W(1)	N(1)	W(2)	172.4(4)	W(1)	N(2)	W(2)	176.2(4)
W(1)	N(3)	C(1)	169.4(8)	W(2)	N(4)	C(2)	172.3(8)
N(3)	C(1)	C(3)	178.7(10)	N(4)	C(2)	C(4)	179(1)
C(1)	C(3)	C(5)	111.6(9)	C(2)	C(4)	C(6)	111.6(8)

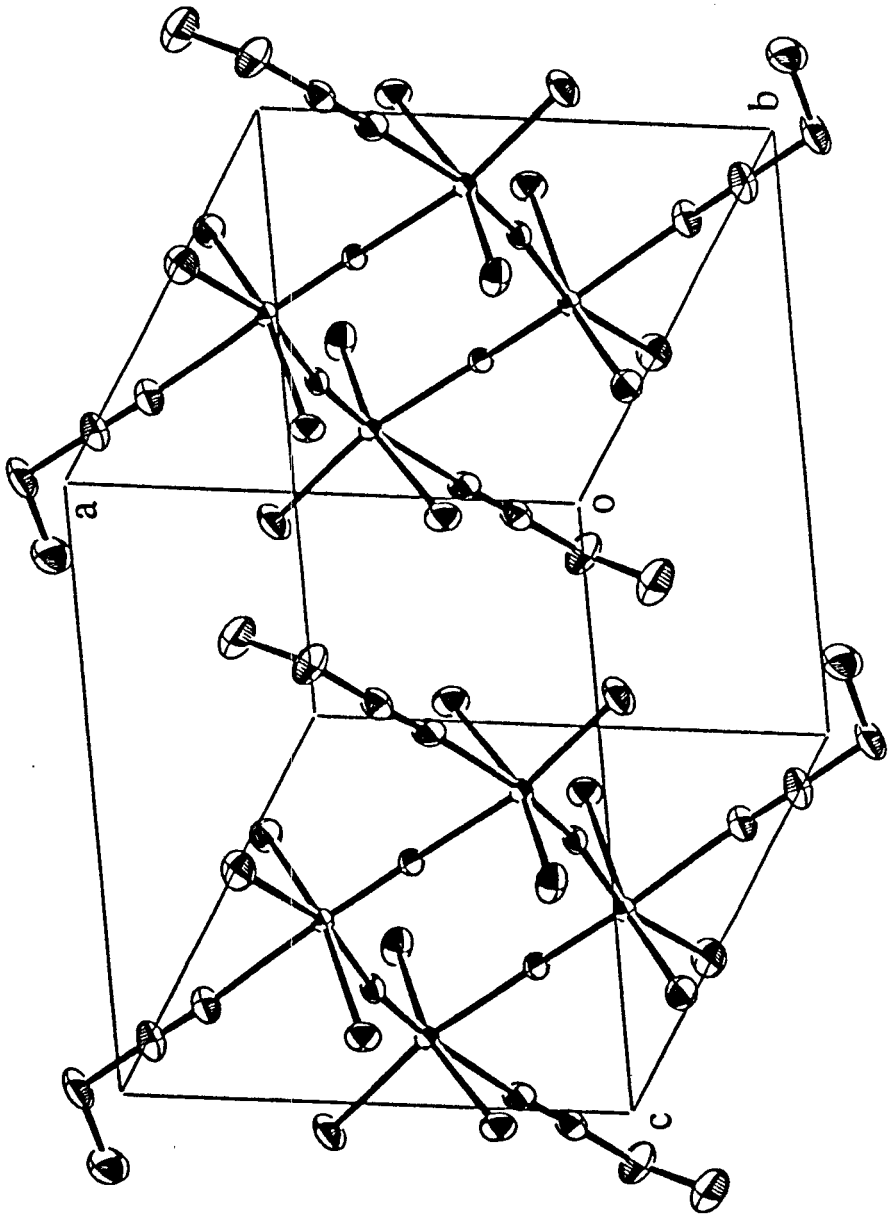

Figure D-1. An ORTEP diagram of the unit cell for $[WNCl_3 \cdot NCCH_2CH_3]_4$.

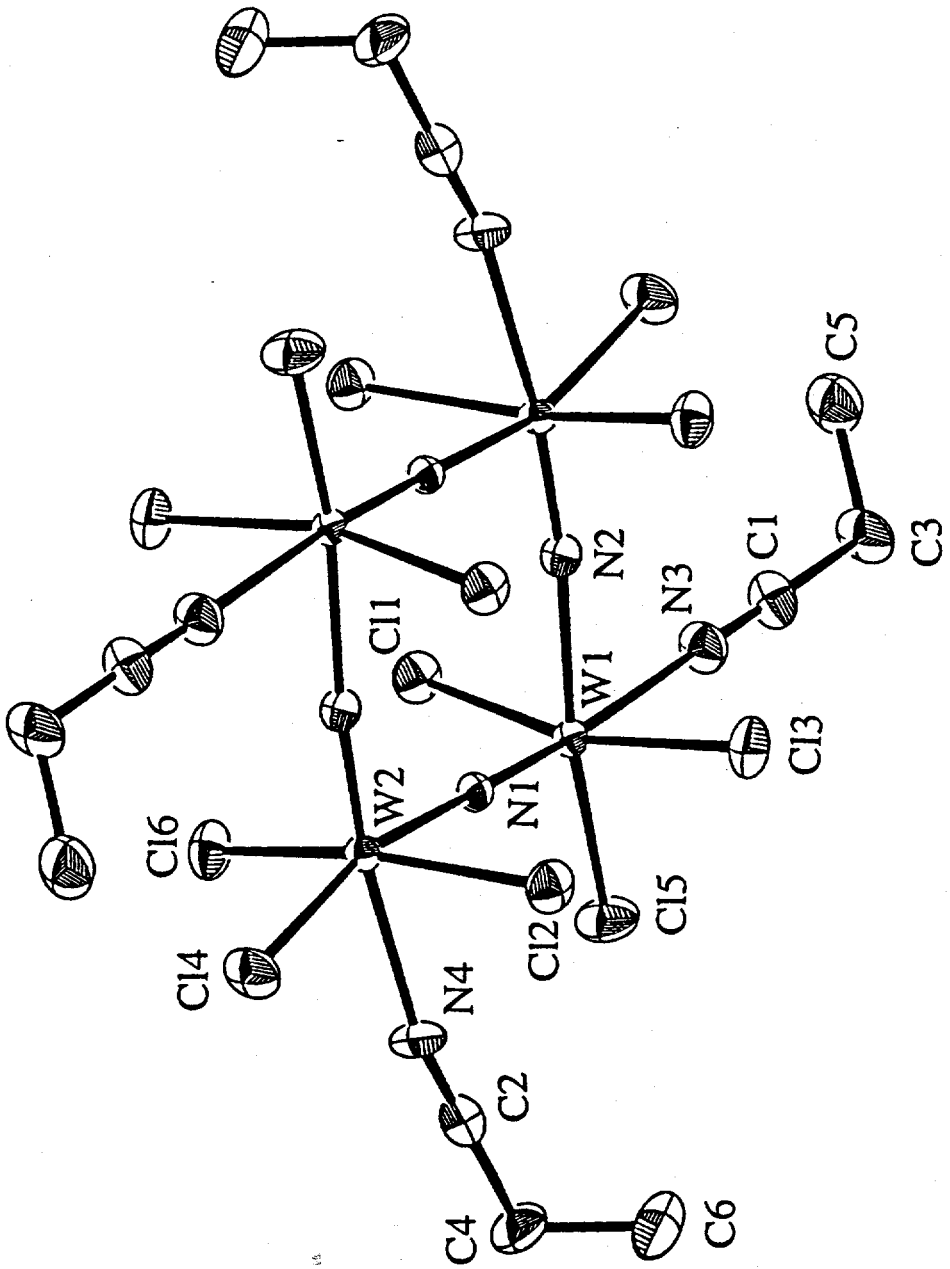

Figure D-2. The molecular structure of $[WNCl_3 \cdot NCCH_2CH_3]_4$.

REFERENCES

1. (a) Yih, S. W. H.; Wang, C. T. *Tungsten: Sources, Metallurgy, Properties, and Applications*, Plenum Press, New York, **1979**.

   (b) Swift, R. A. ed.; *Research of Chrome-Moly Steels*, American Society of Mechanical Engineers, New Yok, **1984**.

2. Deaton, J. C.; Solomon, E. I.; Durfor, C. N.; Wetherbee, P. J.; Burgess, B. K.; Jacobs, D. B. *Biocjem. Biophys. Res. Commun.* **1984**, *121*, 1042.

3. Stein, A.; Keller, S. W.; Mallouk, T. E. *Science*, **1993**, *259*, 1558.

4. (a) Draganjac, M.; Rauchfuss, T. B. *Angew. Chem. Int. Ed. Engl.* **1985**, *24*, 742.

   (b) Böttcher, P. *Angew. Chem. Int. Ed. Engl.* **1988**, *27*, 759.

   (c) Rouxel, J. *Acc. Chem. Res.* **1992**, *25*, 328.

   (d) Dhingra, S.; Kanatzidis, M. G. *Science*, **1992**, *258*, 1769.

5. Nenoff, T. M.; Harrison, W. T. A.; Gier, T. E.; Stucky, G. D. *J. Am. Chem. Soc.* **1991**, *113*, 378.

6. Jacobson, A. J. *Solid State Chemistry Compounds*, Cheetham, A. K.; Day, P. Eds. Claredon Press, **1992**, 182.

7. (a) Baxter, D. V.; Chisholm, M. H.; Gama, G. J.; DiStasi, V. F.; Hector, A. L.; Parkin, I. P. *Chem. Mater.* **1996**, *8*, 1222.

(b) Holl, M. M. B.; Wolczanski, P. T.; Proserpio, D.; Bielecki, A.; Zax, D. B. *Chem. Mater.* **1996**, *8*, 2468.

8. (a) Vennos, D. A.; Badding, M. E.; DiSalvo, F. J. *Inorg. Chem.* **1990**, *29*, 4059.
(b) Elder, S. H.; Doerrer, L. H.; DiSalvo, F. J.; Parise, J. B.; Guyomard, D; Tarascon, J. M. *Chem. Mater.* **1992**, *4*, 928.
9. (a) Jacobs, H.; Niewa R. *Eur. J. Solid State Inorg. Chem.* **1994**, *31*, 105.
(b) Rauch, P. E.; DiSalvo, F. J.; Brese, N. E.; Partin, D. E.; O'Keeffe, M. *J. Solid State Chem.* **1994**, *110*, 162.
10. Subramanya Herle, P.; Hegde, M. S.; Vasanthacharya, N. Y.; Gopalakrishnan,J.; Subbanna, G. N. *J. Solid State Chem.* **1994**, *112*, 208.
11. Bem, D. S.; Olsen, H. P.; zur Loye, H. *Chem. Mater.* **1995**, *7*, 1824.
12. Subramanya Herle, P.; Vasanthacharya, N. Y.; Hegde, M. S.; Gopalakrishnan, J. *J. Alloys Comp.* **1995**, *217*, 22.
13. Bem, D. S.; Lampe-önnerud, C. M.; Olsen, H. P.; zur Loye, H. *Inorg. Chem.* **1996**, *36*, 581.
14. (a) Niewa, R.; Jacobs H. *J. Alloys Comp.* **1996**, *233*, 61.
(b) Niewa, R.; Jacobs H. *J. Alloys Comp.* **1996**, *234*, 171.
15. Lyutaya, M. D. *Soviet Powder Metall. Metal Cer.* **1979**, 190.
16. Lakhtin, Yu. M.; Kogan, Ya, D.; Borovskaya, T. M.; Solodkin, G. A. *Russ. Metall.* **1979**, *4*, 158.

17. Toth, L. E. *Transition Metal Carbides and Nitrides*, Academic Press, NY, **1971**.

18. Brese, N. E.; O'Keeffe, M. *Structure and Bonding*, **1992**, *79*, 307.

19. Khirtrova, V. I. *Soviet Phys. Cryst.* **1962**, *6(4)*, 439.

20. Fix, R. M.; Gordon, R. G.; Hoffman, D. M. *J. Am. Chem. Soc.* **1990**, *112*, 7833.

21. Schönberg, N. *Acta Chemica Scandinavica*, **1954**, *8*, 204.

22. Hector, A. L.; Parkin, I. P. *Chem. Mater.* **1995**, *7*, 1728.

23. Torardi, C. C.; McCarley, R. E. *J. Am. Chem. Soc.* **1979**, *101*, 3963.

24. Schimek, G. L. *Ph. D. Dissertation*, Iowa State University, 1993.

25. Gall, P.; Gougeon, P. *Acta Cryst.* **1992**, *C48*, 1915.

26. Torardi, C. C.; Fecketter, C.; McCarroll, W. H.; DiSalvo, F. J. *J. of Solid State Chem.* **1985**, *60*, 332.

27. Moni, A.; Subramanian, M. A.; Clearfield, A.; DiSalvo, F. J.; McCarroll, W. H. *J. of Solid State Chem.* **1987**, *66*, 136.

28. Gougeon, P.; Gall, P.; McCarley, R. E. *Acta Cryst.* **1991**, *C47*, 1585.

29. (a) Gougeon, P.; Gall, P.; Sergent, M. *Acta Cryst.* **1991**, *C47*, 421.
(b) Gougeon, P.; Gall, P. *Acta Cryst.* **1994**, *C50*, 1183.

30. Gougeon, P.; Gall, P.; McCarley, R. E. *Acta Cryst.* **1991**, *C47*, 2026.

31. Gall, P.; Gougeon, P. *Acta Cryst.* **1993**, *C49*, 659.

32. Gall, P.; Toupet, L.; Gougeon, P. *Acta Cryst.* **1993**, *C49*, 1580.

33. Leligny, H.; Ledesert, M.; Labbe, Ph.; Raveau, B.; McCarroll, W. H. *J. of Solid State Chem.* **1990**, *87*, 35.

34. Gougeon, P.; McCarley, R. E. *Acta Cryst.* **1991**, *C47*, 241.

35. Ramanujachary, K. V.; Jones, E. B.; Greenblatt, M.; McCarroll, W. H. *J. Solid State Chem.* **1995**, *117*, 261.

36. Carlson, C. D. *Ph. D. Dissertation*, Iowa State University, **1989**.

37. Kerihuel, G.; Gougeon, P. *Acta Cryst.* **1995**, *C51*, 787.

38. Kerihuel, G.; Gougeon, P. *Acta Cryst.* **1995**, *C51*, 1475.

ACKNOWLEDGMENTS

I would like to express my sincere appreciation and thanks to Dr. Robert E. McCarley for his guidance and instruction during my graduate years at Iowa State University. Our discussions were always fruitful and motivating. His encouragement and patience helped me to overcome many difficult times in the past five years. Thanks, Doc.

I would also like to thank the past and present members of the McCarley group (George L. Schimek, Xiaobing Xie, and Eylem J. Cahit). Special appreciation goes to Shane J. Hilsenbeck for his generous assistance in many ways.

This research would not have been possible without the aid of the following people and their expertise:

Dr. Robert Jacobson for X-ray crystallography

James Anderegg for X-ray photoelectron spectroscopy

Jerome Ostenson for magnetic susceptibility measurements

Dr. Gordon Miller for EHMO calculations

I would like to thank my family for the support and love they have shown me through telephone and letters from thousands miles away at the other part of the earth. I would also like to thank the many friends I have gained during these years in Ames.

You will always be in my thoughts and memories.

Finally, I am extremely grateful for the love and support of my beautiful wife, Songyan Deng. I will always remember her encouragement, patience and faith during our days in Ames.

This work was performed at the Ames Laboratory under Contract No. W-7405-Eng-82 with the U. S. Department of Energy. The United States government has assigned the DOE Report number IS-T 1829 to this thesis.